Lecture Notes in Applied and Computational Mechanics 84

Peter Wriggers
Thomas Lenarz *Editors*

Biomedical Technology

Modeling, Experiments and Simulation

Springer

Lecture Notes in Applied and Computational Mechanics

Volume 84

Peter Wriggers · Thomas Lenarz
Editors

Biomedical Technology

Modeling, Experiments and Simulation

Springer

Editors
Peter Wriggers
Institute of Continuum Mechanics
Leibniz Universität Hannover
Hannover
Germany

Thomas Lenarz
Hals-Nasen-Ohrenklinik
Medical School Hannover
Hannover
Germany

ISSN 1613-7736 ISSN 1860-0816 (electronic)
Lecture Notes in Applied and Computational Mechanics
ISBN 978-3-319-59547-4 ISBN 978-3-319-59548-1 (eBook)
DOI 10.1007/978-3-319-59548-1

Library of Congress Control Number: 2017941488

Printed on acid-free paper

This Springer imprint is published by Springer Nature
The registered company is Springer International Publishing AG
The registered company address is: Gewerbestrasse 11, 6330 Cham, Switzerland

The Choice of a Performance Indicator of Release in Transdermal Drug Delivery Systems

Giuseppe Pontrelli and Laurent Simon

Abstract An effective time constant for first-order processes is defined to capture the dynamics of systems represented by partial differential equations. In this chapter, the methodology is applied to passive and electrically assisted drug controlled transdermal delivery devices in two case studies. The analysis, which is carried out using Laplace-transformed variables, results in a first-order approximation and does not require time-domain solutions. Numerical experiments are included to illustrate the effectiveness of the index under different conditions and to estimate the time it takes to establish a steady-state flux across the membrane.

1 Introduction

Traditional transdermal drug delivery (TDD) systems are based on the transport of therapeutic agents across the skin by passive diffusion. Despite being the subject of extensive research over the years because of its potential advantages, the exact release mechanism remains unclear in some cases and it is often difficult to predict the drug kinetics accurately [1, 2]. The solutes which can be administered by transdermal route are limited to molecules of low molecular weight, due to the excellent barrier properties of the stratum corneum, the outermost layer of the epidermis [3]. To increase skin's drug transport and overcome this limitation, innovative technologies have been developed, some of them based on the use of electrical current (*iontophoresis*). In these electrically assisted systems, an applied potential of low intensity ($\approx 1V$) generates an additional driving force for the drug motion in the skin [4, 5].

G. Pontrelli (✉)
IAC-CNR, Via Dei Taurini 19, Roma, Italy
e-mail: giuseppe.pontrelli@gmail.com

L. Simon
New Jersey Institute of Technology, Newark, NJ, USA
e-mail: laurent.simon@njit.edu

P. Wriggers and T. Lenarz (eds.), *Biomedical Technology*, Lecture Notes in Applied and Computational Mechanics 84, DOI 10.1007/978-3-319-59548-1_4

The application of transdermal patches for accurate delivery of medicaments to their target sites is another possible non-invasive technology: the drug is initially stored in the vehicle, a porous polymeric reservoir having an impermeable backing at one side and an adhesive in contact with the skin at the other side, and is subsequently released in a controlled manner [6, 7]. Compared to conventional TDD products, the rational design of these novel drug delivery devices poses further challenges, such as the complex mechanisms and the unknown significance of process parameters. Additional factors include the device polymeric microstructure characteristics and properties of the electric field.

In the absence of experimental data, mathematical modelling of TDD allows to predict drug release from the vehicle and its transport into the target tissue. The framework also offers insights into the factors governing drug delivery and provide quantitative relationships between drug concentration, or the delivery rate, and some key design drug/vehicle properties [8]. For traditional TDD, the coupling between the diffusion process in the reservoir and in the target tissue has been considered in [6, 9]. In the majority of TDD models, a constant flux enters the target tissue and the role of the reservoir finite capacity is neglected [10].

Moreover, the above models assume that the skin is homogeneous and ignore its composite structure. In fact, it is well accepted that the skin is an inhomogeneous medium, composed of several layers with different thickness and physico-chemical-electrical properties (Fig. 1). This aspect has a crucial importance since the drug transport critically relates to the local diffusive properties and, even more importantly in iontophoresis, the potential field relies on the layer-dependent electrical conductivities. The multi-layer structure of the biological media and other related issues have been addressed in other papers [11] and in a recent work, where a model of iontophoretic drug release from a vehicle into a multi-layered dermal tissue is presented [12]. However, even in situations where the transport phenomena are well represented mathematically, the need exists to develop analytical tools or simple indicators to extract meaning from the model and the data. These tools will make possible to answer certain questions, such as how long it takes to attain a therapeutic flux, or what processing conditions need to be adjusted and by how much, in order to reach a desired delivery rate without solving the full differential equations. Furthermore, when a full mathematical representation is not available, or is too complicated for being of practical use, simple performance indicators are required to elucidate the main transport mechanisms and identify the most critical components in TDD.

Among several mathematical techniques available for control systems analysis, Laplace transform and linearization are frequently applied to describe a process dynamics through an effective time constant (ETC)(denoted by t_{eff}) [13]: this represents a useful indicator of the time elapsed before reaching a steady state. The existence of a single ETC is of great importance in the design of drug delivery systems, because it would allow product manufacturers to tune specific properties to ensure that a constant release is reached at a specific time [7]. The problem is to find a formal definition of t_{eff} which makes the index precise for a general dynamical

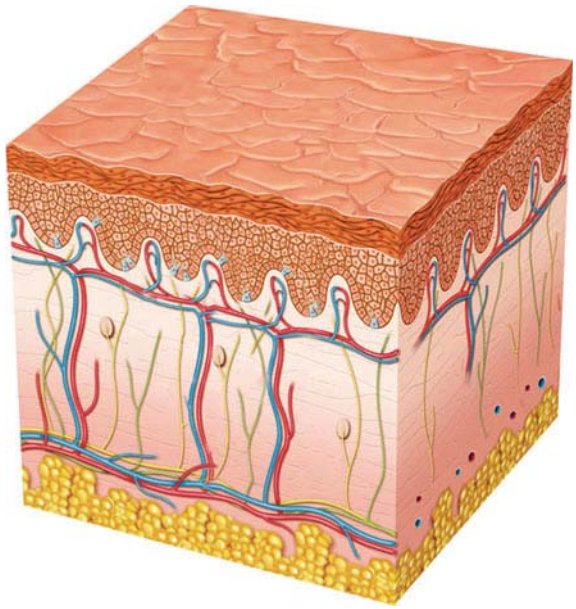

Fig. 1 An anatomic representation of the skin, composed by three main layers: epidermis (approximately 100 μm thick), dermis (between 1 and 3 mm thick, highly vascularized) and a subcutaneous tissue. The epidermis is divided into sub-layers where the stratum corneum (approximately 10 μm thick) is the outermost layer and is the major barrier to the drug migration, being composed of densely packed cells, with a typical *brick and mortar* structure. Each skin layer, due to its histological composition, has a different influence on the drug transport mechanism

system, no matter how complicated it is, even in cases when the time-dependence departs markedly from a simple exponential form. For a practical and useful definition, it must also be possible to compute t_{eff} in a simple and straightforward manner to enable different convective-diffusive systems to be compared on a common basis. Our goal is to relate ETC to the model parameters of a TDD device. This allows, with the aid of a single index, to understand the role of key factors influencing the release of active pharmaceutical ingredients and to assess the time drug reaches a target steady-state flux and to optimize the release performance.

The chapter is organized as follows. In Sect. 2, we introduce the concept of the ETC and its use in a general framework. In Sect. 3 the one-layer model in TDD is presented, and in Sect. 4 the computation of ETC is carried out. The mathematical problem in a multi-layered model is addressed in Sect. 5 followed by the correspondent ETC derivation (Sect. 6). Finally in Sect. 7 some numerical estimates of ETC and drug flux in the various cases, are presented and discussed for a realistic range of parameters and typical drugs.

2 The Concept of an Effective Time Constant: Definition and Applications

The introduction of a dynamic metric for controlled-release systems stems from the need to link the performance of formulations to measurable physico-chemical features of the drug and vehicle. For example, in transdermal heat-enhanced devices, manufacturers have the opportunity to design products that address the needs of patients suffering from breakthrough cancer pain. The idea is to dramatically tighten the pain-relief gap by triggering a prompt onset of drug effect. Although opioids are usually administered intravenously, there has been a growing interest in using physical enhancers to make transdermal patches designed to meet unique treatment protocols required by cancer patients. Preliminary studies, conducted by Ashburn et al., have shown some of the benefits of the application of local heat to transdermal fentanyl patches [14]. These researchers noticed that, when applying these patches with no controlled heat, attaining a steady-state blood level of the medicament may require a long time. One the contrary, an increase observed in the serum concentration immediately after the application of controlled heat, suggests that such technologies may prove effective in the delivery of analgesia [14]. A computational method to estimate the onset of action based on the properties of the active and inactive pharmaceutical ingredients, would be very useful in this case. It has also been shown that the period elapsed to reach 98% of the steady-state flux, defined by four times the first time constant, is related to the properties of the delivery system, although no analytical expression is available [15].

The ability of iontophoresis to deliver medicaments through the skin and quickly establish a therapeutic level has been studied. Song et al. [16] developed an alternating current technique to increase the permeation rate of urea and decrease the lag time in the human epidermal membrane. These researchers suggested that the design of iontophoretic drug-delivery devices would improve, considerably, if the transport lag time was well characterized and flux variability decreased [16]. Although the controlled-release community has expressed special interest in controlling the factors that delay the onset of the steady-state release rate [17], early efforts used compartmental models of transdermal iontophoretic transport [18]. This approach provides limited mechanistic insight and makes it difficult to extrapolate the findings to new iontophoretic products.

Laplace transform and linearization are commonly applied to examine the dynamic responses of many processes. These procedures help control engineers and process designers determine relevant characteristic parameters which affect the transient behavior of a plant [19]. For example, let us consider a storage tank with inlet and outlet flows: the time elapsed before reaching a steady-state liquid level, after changing the inlet flow rate, is related to the tank area and the flow resistance in the outlet pipe. The transfer function reveals that the product of these two factors represents the process time constant. Based on the success of these techniques, there have been significant efforts made, by researchers, toward implementing these tools to best describe the dynamics of diffusion [13]. A similar approach is considered

in this work to derive design equations that connect ETC to key properties. These features can be use by manufacturers of controlled-released systems to guarantee accurate release of active pharmaceutical ingredients to a selected site.

To assess the suitability of the method, let us start with a first-order system [19]:

$$\tau_p \frac{dy}{dt} + y = K_p u(t) \tag{1}$$

where τ_p (otherwise called t_{eff}) and K_p indicate the time constant and steady-state gain of the process, respectively; u and y are the input and output variables. While K_p is the ratio of the ultimate response (y_{ss}) to the size of a step change in u, τ_p is a measure of the time it takes to reach y_{ss}. The gain K_p determines the sensitivity of a system. For example, consider a process where saturated steam is supplied to heat the liquid in a vessel. A K_p value of 7 °F/(lb/min) suggests that an increase of 1.0 lb/min in the steam mass flow rate is necessary to raise the liquid temperature by 7 °F. It can be shown that y has achieved 63.2% of its steady-state value after one time constant. At $t_{res} = 4\tau_p$ (called the *response time*), y is at 98% of its ultimate value. In the previous example, the response time denotes the period elapsed before the temperature changes by 7 °F. By Eq. (1), using the Laplace variable s, often used to analyze the dynamics of linear systems, the response becomes:

$$Y(s) = \frac{K_p}{\tau_p s + 1} U(s) \tag{2}$$

The variables Y and U represent the Laplace transforms u and y assuming that $y(0) = u(0) = 0$.

This concept of a single time constant to describe a process dynamics is extended to systems in which the variable of interest can be approximated by a series of the form:

$$\chi(\mathbf{x}, t) = \sum_{n=1}^{\infty} f_n(\mathbf{x}) e^{-\lambda_n t} \tag{3}$$

where $\lambda_n = 1/t_n$ and f_n is a function of the space $\mathbf{x}$. The numbers t_n denote the characteristic time constants with $t_n > t_m$ or $\lambda_n < \lambda_m$ for $n < m$. In general, the system dynamics is represented by the first λ_n values. To use a single time constant that estimates how fast $\chi(\mathbf{x}, t)$ approaches the equilibrium $\chi_{eq}(\mathbf{x})$, a first-order moment with a normalized probability density function $\Omega(\mathbf{x}, t)$ is applied:

$$t_{eff}(\mathbf{x}) = \int_0^{\infty} t\Omega(\mathbf{x}, t)\, dt \tag{4}$$

where

$$\Omega(\mathbf{x},t)=\frac{\chi_{eq}(\mathbf{x})-\chi(\mathbf{x},t)}{\int_0^{\infty}\left(\chi_{eq}(\mathbf{x})-\chi(\mathbf{x},t)\right)dt}$$

The properties of Laplace transforms can be used to write ETC defined in Eq. (4) in terms of s [7]:

$$t_{eff}(\mathbf{x})=\frac{\lim_{s\to 0}\left(\frac{\chi_{eq}(\mathbf{x})}{s^2}+\frac{d\bar{\chi}}{ds}(\mathbf{x},s)\right)}{\lim_{s\to 0}\left(\frac{\chi_{eq}(\mathbf{x})}{s}-\bar{\chi}(\mathbf{x},s)\right)} \tag{5}$$

with $\bar{\chi}(\mathbf{x},s)$ the Laplace transform of $\chi(\mathbf{x},t)$. An inspection of Eq. (4) shows that $t_{eff}(\mathbf{x})$ is guaranteed to have a positive value as long as the difference $\frac{\chi_{eq}(\mathbf{x})}{s}-\bar{\chi}(\mathbf{x},t)$ does not change sign. Although there are other performance indicators (e.g., lag time) that have been defined to describe process dynamics [7], ETC remains the most effective indicator for our purposes. In the following, we apply the previous concepts to a one and multi-layered cases. The ETC is defined and computed for both systems.

3 A One-Layer Model for TDD

Let us consider a TDD system, where the skin is modeled as a planar membrane in contact with an infinite reservoir (i.e., constant drug concentration) and a receiver chamber. Because most of the mass transfer occurs along the direction normal to the skin surface, we restrict our study to a simplified 1D model. In particular, we consider a Cartesian coordinate and draw a line pointing inwards which crosses the vehicle and the skin. The skin surface is located at $x=0$; $x=x_1$ is the thickness of the SC (Fig. 2). Here, diffusion is assumed to take place only in the stratum corneum (SC) instead of the full-thickness skin, due to the formidable barrier posed by this layer. Permeation through the SC is the rate-limiting step [8]. We use $c\approx 0$ at the SC limit $x=x_1$ to show rapid removal of the drug from the interface between the SC and the viable epidermis by rapid diffusion followed by absorption by the blood vessels [20].

Iontophoretic transport

To promote TDD, an electric field is locally applied in the area where the therapeutic agent has to be released (*iontophoresis*): for example, the anode is at $x=0$ and the cathode is at $x=x_1$. Let Ψ_0 and Ψ_1 ($\Psi_0>\Psi_1$) be the correspondent applied potential at the endpoints (Fig. 2). By mass conservation, the drug concentration[1] satisfies the following equation:

[1] A mass volume-averaged concentration $c_1(x,t)$ (mg/cm^3) is considered in this chapter.

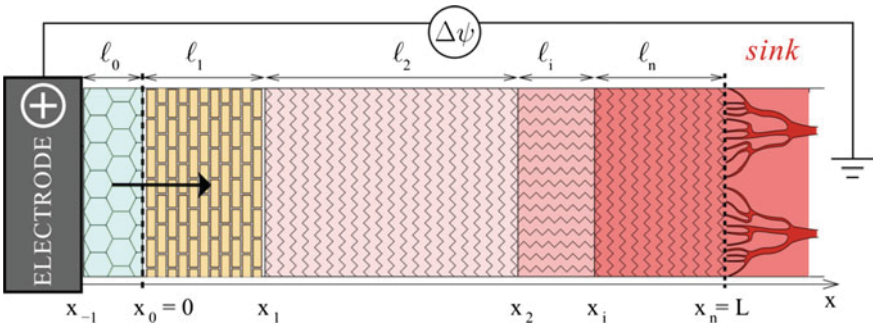

Fig. 2 A diagram of a n-layered tissue ($\ell_1, \ell_2, ..., \ell_n$) with a vehicle ℓ_0. In some cases, the model is confined to SC layer only (Sect. 3), while in a more realistic situation, it includes several layers (Sect. 5) The 1D model is defined along the line normal to the skin surface and extends with a sequence of n contiguous layers from the vehicle interface $x_0 = 0$ up to the skin bound $x_n = L$, where capillaries sweep the drug away to the systemic circulation (sink). In iontophoresis, a difference of potential is applied to facilitate drug penetration across the skin's layers (figure not to scale)

$$\frac{\partial c_1}{\partial t} + \nabla \cdot J_1 = 0 \tag{6}$$

and the mass flux is defined by the Nernst-Planck flux equation [10]:

$$J_1 = -D_1 \nabla c_1 - u_1 c_1 \nabla \phi_1, \tag{7}$$

where ϕ_1 is the electric potential and the convective (electroosmotic) term is omitted. Equation (7) is the generalized Fick's first law with an additional driving force which is proportional to the electric field. The electric mobility is related to the diffusivity coefficient through the Einstein relation:

$$u_1 = \frac{D_1 z F}{RT}, \tag{8}$$

($\mathrm{cm}^2\, V^{-1}\, s^{-1}$), where z ion valence, F the Faraday constant, R the gas constant, T the absolute temperature. The boundary conditions are:

$$c_1 = c_{10} \qquad \text{at} \quad x = 0 \tag{9}$$

$$c_1 = 0 \qquad \text{at} \quad x = x_1 \tag{10}$$

where c_{10} is related to the vehicle concentration c_0 by $c_0 = K_0^1 c_{10}$ with K_0^1 the reservoir/skin partition coefficient. The Eq. (10) arises because, in deep skin, drug is uptaken by capillary network and is lost in the systemic circulation: we refer to this as systemically absorbed drug.

The initial conditions is set as:

$$c_1(x,0) = 0 \tag{11}$$

The electric potential field

To solve Eqs. (6)–(8) in $[0, x_1]$, we first seek a solution of the Poisson equation [10]:

$$\begin{aligned} &\nabla \cdot (\sigma_1 \nabla \phi_1) = \rho(x) \simeq 0 \\ &\phi_1 = \Psi_0 \qquad \text{at} \quad x = 0 \\ &\phi_1 = \Psi_1 \qquad \text{at} \quad x = x_1 \end{aligned} \tag{12}$$

with $\sigma_1(\,\mathrm{cm}^{-1}\,\Omega^{-1})$ the skin electrical conductivity and $\rho(x)$ is the charge density over the permittivity [4]. It is straightforward to verify that the exact solution of the problem (12) is

$$\phi_1(x) = a_1 x + b_1 \tag{13}$$

with the expressions of a_1 (V/cm) and $b_1(V)$ given in Sect. 7.

4 Computation of the ETC for a One-Layer Skin Model

For the system described by Eqs. (6)–(11), the goal is to determine the period elapsed before reaching a steady-state flux by first estimating the ETC. Therefore, the cumulative amount of drug released at $x = x_1$ and into the systemic circulation is also an increasing function:

$$M(t) = \int_0^t -D\frac{\partial c_1}{\partial x}(x_1, \tau)d\tau \tag{14}$$

and, by definition of a monotonic function, the time derivative of $M(t)$ (e.g., the flux at $x = x_1$) does not change sign. It starts at 0 and reaches a steady-state value.

After applying the definition of the Laplace transform to c_1, we get

$$\bar{c}_1(x,s) = \int_0^\infty c_1(x,t)\exp(-st)dt \tag{15}$$

where $\bar{c}_1(x,s)$ is the Laplace transform of $c_1(x,t)$. Substituting $\bar{c}_1(x,s)$ into Eqs. (6)–(7) leads to the following solution:

$$\bar{c}_1(x,s) = k_1 \exp\left[\frac{1}{2}x\left(-\frac{\gamma_1}{D_1} - \frac{\sqrt{\gamma_1^2 + 4D_1 s}}{D_1}\right)\right] + k_2 \exp\left[\frac{1}{2}x\left(\frac{\sqrt{\gamma_1^2 + 4D_1 s}}{D_1} - \frac{\gamma_1}{D_1}\right)\right] \tag{16}$$

with $\gamma_1 = u_1 a_1$. Equation (16) is solved for k_1 and k_2 after imposing the boundary conditions (9) and (10). These integration constants are replaced in (16) to give $\bar{c}_1(x, s)$. An expression for the flux at $x = x_1$ in terms of s gives

$$J_1(s) = \frac{c_{10}\sqrt{\gamma_1^2 + 4D_1 s}\ \exp\left[\dfrac{x_1\left(\sqrt{\gamma_1^2 + 4D_1 s} - \gamma_1\right)}{2D_1}\right]}{s\left[\exp\left(\dfrac{x_1\sqrt{\gamma_1^2 + 4D_1 s}}{D_1}\right) - 1\right]} \tag{17}$$

The ETC, obtained from Eq. (4), and the steady-state flux are

$$t_{eff} = \frac{\gamma_1^2 {x_1}^2\left[2\mathrm{csch}^2\left(\dfrac{\gamma_1 x_1}{2D_1}\right) + 1\right] - 2\gamma_1 D_1 x_1 \coth\left(\dfrac{\gamma_1 x_1}{2D_1}\right) - 4D_1^2}{2\gamma_1^2\left[\gamma_1 x_1 \coth\left(\dfrac{\gamma_1 x_1}{2D_1}\right) - 2D_1\right]} \tag{18}$$

and

$$J_{1eq} = \frac{c_{10}\gamma_1}{\exp\left(\dfrac{\gamma_1 x_1}{D_1}\right) - 1} \tag{19}$$

respectively. Note that

$$\lim_{\gamma_1 \to 0} t_{eff} = \frac{7{x_1}^2}{60D_1} \qquad \lim_{\gamma_1 \to 0} J_{1eq} = \frac{c_{10}D_1}{x_1}$$

recover the expressions for the passive (simple) diffusion [7].

5 A Multi-layer Model for TDD

The skin has a typical composite structure, constituted by a sequence of contiguous layers of different physical properties and extensions. To be more realistic, let us generalize the previous model and consider the skin made of several layers of thicknesses $l_1, l_1, ..., l_n$, each treated as a macroscopically homogeneous porous medium. Therefore, a set of intervals $[x_{i-1}, x_i]$, $i = 1, \ldots, n$ ($x_n = L$) are defined (Fig. 2).

Iontophoretic transport

As in the case of the one-layer model, the concentration satisfies the following equation:

$$\frac{\partial c_i}{\partial t} + \nabla \cdot J_i = 0 \tag{20}$$

and in each layer i the mass flux is defined by the Nernst-Planck flux equation [10]:

$$J_i = -D_i \nabla c_i - u_i c_i \nabla \phi_i, \qquad u_i = \frac{D_i z F}{RT}, \qquad i = 1, \dots, n \tag{21}$$

where ϕ_i is the electric potential in layer i. The boundary conditions are:

$$c_1 = c_{10} \quad \text{at} \quad x = 0 \tag{22}$$

$$c_n = 0 \quad \text{at} \quad x = x_n \quad \text{(sink condition due to the capillary washout)} \tag{23}$$

At the layer interfaces, we impose continuity of mass fluxes and ratio of equilibrium concentrations equal to partition coefficients:

$$J_i = J_{i+1} \qquad c_i = K_{i,i+1}\, c_{i+1} \qquad \text{at} \quad x = x_i, \qquad i = 1, 2, \dots, n-1 \tag{24}$$

The initial conditions are:

$$c_i(x, 0) = 0 \qquad i = 1, 2, \dots, n \tag{25}$$

The electric potential field

In this multi-layer model, the potential is the solution of the multiple Poisson equations [10]:

$$\begin{aligned} &\nabla \cdot (\sigma_i \nabla \phi_i) = \rho(x) \simeq 0 \qquad i = 1, \dots, n \\ &\phi_1 = \Psi_0 \qquad \text{at} \quad x = 0 \\ &\phi_n = \Psi_1 \qquad \text{at} \quad x = x_n \end{aligned} \tag{26}$$

with $\sigma_i(\,\mathrm{cm}^{-1}\,\Omega^{-1})$ the electrical conductivities in the layer i. At the interfaces we assume an electrically perfect contact and we impose continuity of potential and fluxes:

$$-\sigma_i \nabla \phi_i = -\sigma_{i+1} \nabla \phi_{i+1} \qquad \phi_i = \phi_{i+1} \qquad \text{at} \quad x = x_i \qquad i = 1, \dots, n-1 \tag{27}$$

It is straightforward to verify that the exact solution of the problem (26)–(27) is

$$\phi_i(x) = a_i x + b_i \qquad i = 1, \dots, n \tag{28}$$

with the expressions of $a_i\,(\mathrm{V/cm})$ and $b_i(V)$ are computed as in [12] (see Sect. 7).

6 Computation of the ETC for a Multi-layer Skin Model

For simplicity, a three-layer skin model ($n = 3$) is studied. The governing Eqs. (20)–(21) read:

$$\frac{\partial c_1}{\partial t} = D_1 \frac{\partial^2 c_1}{\partial x^2} + \frac{\partial}{\partial x}\left(u_1 c_1 \frac{\partial \phi_1}{\partial x}\right) \qquad \text{in } [0, x_1] \tag{29}$$

$$\frac{\partial c_2}{\partial t} = D_2 \frac{\partial^2 c_2}{\partial x^2} + \frac{\partial}{\partial x}\left(u_2 c_2 \frac{\partial \phi_2}{\partial x}\right) \qquad \text{in } [x_1, x_2] \tag{30}$$

$$\frac{\partial c_3}{\partial t} = D_3 \frac{\partial^2 c_3}{\partial x^2} + \frac{\partial}{\partial x}\left(u_3 c_3 \frac{\partial \phi_3}{\partial x}\right) \qquad \text{in } [x_2, L] \tag{31}$$

The equilibrium partition relations at the boundaries are

$$c_0 = K_{0,1} c_1 \qquad \text{at} \quad x = 0 \tag{32}$$

$$c_1 = K_{1,2} c_2 \qquad \text{at} \quad x = x_1 \tag{33}$$

$$c_2 = K_{2,3} c_3 \qquad \text{at} \quad x = x_2 \tag{34}$$

The flux continuity equations at the boundaries are

$$D_1 \frac{\partial c_1}{\partial x} + u_1 c_1 \frac{\partial \phi_1}{\partial x} = D_2 \frac{\partial c_2}{\partial x} + u_2 c_2 \frac{\partial \phi_2}{\partial x} \qquad \text{at} \quad x = x_1 \tag{35}$$

$$D_2 \frac{\partial c_2}{\partial x} + u_2 c_2 \frac{\partial \phi_2}{\partial x} = D_3 \frac{\partial c_3}{\partial x} + u_3 c_3 \frac{\partial \phi_3}{\partial x} \qquad \text{at} \quad x = x_2 \tag{36}$$

At the dermis/capillary interface, we have

$$c_3 = 0 \qquad \text{at} \quad x = L \tag{37}$$

Following a method similar to the one described in Sect. 4, the Laplace transformed concentrations are:

$$\bar{c}_1(x, s) = k_1 \exp\left[\frac{1}{2}x\left(-\frac{\gamma_1}{D_1} - \frac{\sqrt{\gamma_1^2 + 4D_1 s}}{D_1}\right)\right] + k_2 \exp\left[\frac{1}{2}x\left(\frac{\sqrt{\gamma_1^2 + 4D_1 s}}{D_1} - \frac{\gamma_1}{D_1}\right)\right]$$

$$\bar{c}_2(x, s) = k_3 \exp\left[\frac{1}{2}x\left(-\frac{\gamma_2}{D_2} - \frac{\sqrt{\gamma_2^2 + 4D_2 s}}{D_2}\right)\right] + k_4 \exp\left[\frac{1}{2}x\left(\frac{\sqrt{\gamma_2^2 + 4D_2 s}}{D_2} - \frac{\gamma_2}{D_2}\right)\right]$$

and

$$\bar{c}_3(x, s) = k_5 \exp\left[\frac{1}{2}x\left(-\frac{\gamma_3}{D_3} - \frac{\sqrt{\gamma_3^2 + 4D_3 s}}{D_3}\right)\right] + k_6 \exp\left[\frac{1}{2}x\left(\frac{\sqrt{\gamma_3^2 + 4D_3 s}}{D_2} - \frac{\gamma_3}{D_3}\right)\right]$$

with $\gamma_1 = u_1 a_1$, $\gamma_2 = u_2 a_2$ and $\gamma_3 = u_3 a_3$. The integration constants k_i with $i = 1, ..., 6$ are obtained after solving Eqs. (32)–(37) in the Laplace domain. Using these results, expressions for ETC and the steady flux are derived at $x = L$. The functions are not shown here because of page limitation, but the numerical results are given in the next section.

7 Computational Results

To evaluate the dynamic behavior of a transdermal drug delivery, with a possible iontophoretic enhancement, an estimate of ETC is made in the one-layer and multi-layer model.

One-layer model

In the case where the skin is modelled by a single layer, we use the following nominal parameters corresponding to the permeation of arginine vasopressin through hairless rat skin [21]:

$$x_1 = 10^{-3}\,\text{cm} \qquad D_1 = 1.1 \times 10^{-11}\,\text{cm}^2/\text{s} \qquad z_1 = +2 \tag{38}$$

With these data at hand, it results: $\text{csch}^2\left(\frac{\gamma_1 x_1}{2D_1}\right) \approx 0$ and $\coth\left(\frac{\gamma_1 x_1}{2D_1}\right) \approx -1$, and Eq. (18) reduces to:

$$t_{eff} \approx \frac{\gamma_1^2 x_1^2 + 2\gamma_1 D_1 x_1}{-2\gamma_1^2(\gamma_1 x_1 + 2D_1)} \approx -\frac{1}{2}\frac{x_1}{\gamma_1}$$

Similarly, in Eq. (19), given that $\exp\left(\frac{\gamma_1 x_1}{D_1}\right) \approx 0$, the steady flux velocity at x_1 reduces to:

$$\frac{J_{1eq}}{c_{10}} \approx -\gamma_1$$

Therefore, the dependence of ETC on $\Delta\Psi$ is roughly inversely linear. The steady-state flux is quasi-linear to the DelPhi. Although the procedure yields fairly complex expressions (Eqs. 18 and 19), in the physiological range, a simple dependence on $\gamma_1 = u_1 a_1$ (see Eqs. (8) and (13)) results (Fig. 3).

Multi-layer model

Here, the skin is assumed to be composed of three main layers, the SC, the viable epidermis, and the dermis (Fig. 4). The model parameters are given in Table 1. In the absence of direct measurements, indirect data are inferred from previous studies in literature [22, 23]. Diffusivities depend on the type and size of the transported molecules and are affected of a high degree of uncertainty. Representative values of partition coefficients are listed [21, 24]. The $K_{2,3}$ value of 1.0 was selected because

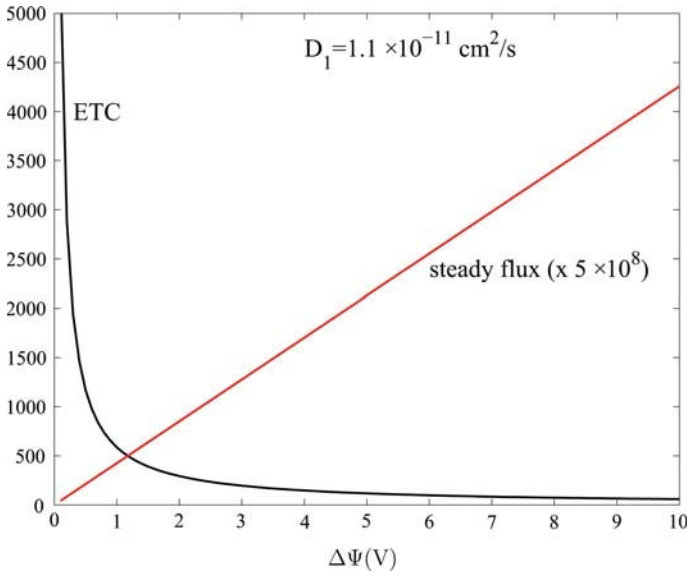

Fig. 3 The near-linear inverse dependence of ETC and the quasi-linear dependence for steady flux J_{1eq}/c_{10} on $\Delta\Psi$ (case one-layer). A similar trend is reported for varying D_1, at a fixed $\Delta\Psi$

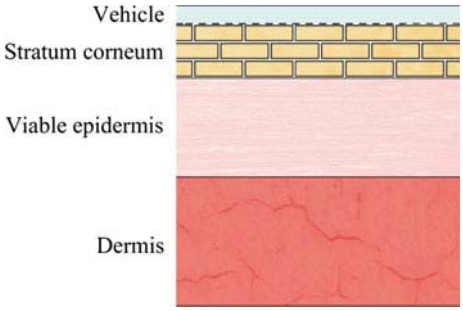

Fig. 4 A schematic section representing the three-layer model (figure not to scale)

Table 1 The parameters used in the simulations for the three-layer model

—	Stratum corneum (SC) (1)	Viable epidermis (2)	Dermis (3)
$l_i = x_i - x_{i-1}$ (cm)	1.75×10^{-3}	3.5×10^{-3}	0.11
D_i (cm^2/s)	10^{-10}	10^{-7}	10^{-7}
σ_i (S/cm)	10^{-7}	10^{-4}	10^{-4}
$K_{i-1,i}$	0.01	2.2	1.0

Table 2 The ETC and steady flux as a function of different currents with $D_1 = 10^{-11}\,\mathrm{cm}^2/\mathrm{s}, D_2 = 10^{-7}\,\mathrm{cm}^2/\mathrm{s}, D_3 = 10^{-7}\,\mathrm{cm}^2/\mathrm{s}$

$\Delta\Psi(V)$	$a_1/a_2/a_3\,(\mathrm{V/cm})$	ETC(s)	$J_{1eq}/c_{10}\,(\mathrm{cm/s})$
0	0/0/0	5.41×10^4	5.71×10^{-7}
1.0	$-538.1/-0.54/-0.54$	3.89×10^4	2.08×10^{-5}
1.5	$-807.2/-0.81/-0.81$	1.22×10^4	3.12×10^{-5}
1.7	$-914.8/-0.91/-0.91$	8.00×10^3	3.54×10^{-5}
2.0	$-1076.3/-1.08/-1.08$	4.10×10^3	4.16×10^{-5}

Table 3 The ETC and steady flux as a function of different diffusivities with $\Delta\Psi = 1.0\,V$

$D_1\,(\mathrm{cm^2 s^{-1}})$	$D_2\,(\mathrm{cm^2 s^{-1}})$	$D_3\,(\mathrm{cm^2 s^{-1}})$	ETC(s)	$J_{1eq}/c_{10}\,(\mathrm{cm/s})$
10^{-11}	10^{-7}	10^{-7}	3.89×10^4	2.08×10^{-5}
2.0×10^{-11}	2.0×10^{-7}	2.0×10^{-7}	1.94×10^4	4.16×10^{-5}
3.0×10^{-11}	3.0×10^{-7}	3.0×10^{-7}	1.30×10^4	6.25×10^{-5}
4.0×10^{-11}	4.0×10^{-7}	4.0×10^{-7}	9.73×10^3	8.33×10^{-5}

the viable epidermis is usually treated as an aqueous tissue nearly equivalent to the dermis [25]. The coefficients a_i of the potential ϕ_i in Eq. (28) have the following expressions:

$$a_1 = -\frac{\Delta\Psi\sigma_2\sigma_3}{G} \qquad a_2 = -\frac{\Delta\Psi\sigma_1\sigma_3}{G} \qquad a_3 = -\frac{\Delta\Psi\sigma_1\sigma_2}{G}$$

where $G = l_3\sigma_1\sigma_2 + l_1\sigma_3(\sigma_2 - \sigma_1) + l_2\sigma_1(\sigma_3 - \sigma_2)$ and $\Delta\Psi = \Psi_0 - \Psi_1$.

The results are shown in Tables 2 and 3. As in the one-layer case, an electrical current—as well as increasing layer diffusivities—promotes a more effective release and enhances the drug flux in a nearly linear way, leading a reduced ETC. Nevertheless, since the thicknesses and compositions of the tissues are different in the one- and three-layer cases, the numerical values of ETC and flux are not directly comparable.

Although the model parameters are subject to some degree of uncertainty, estimation of the ETC is an important tool that can be applied for the successful release of new molecules and the improved delivery of conventional drugs.

8 Conclusions

The dynamic behavior of a finite physical system can often be described by a single relaxation time constant. In this chapter we have defined such an effective time constant as a design tool for transdermal drug release, possibly enhanced by iontophoresis. As a single index of release performance, the ETC has the advan-

tage that it can be evaluated from Laplace transforms without the need of explicit inversions, and can be used to describe the different effective speeds of relaxation of an extended system. Although closed-form expressions of ETC are not always easy to obtain and analyze, ETC has been derived and computed for two case studies: the transdermal drug delivery in one-layer and multi-layer models, with convection terms present in the case of electrically-assisted release.

References

1. M. Prausnitz, R. Langer, Transdermal drug delivery. Nat. Biotech. **26**, 1261–1268 (2008)
2. O. Perumal, S. Murthy, Y. Kalia, Tuning theory in practice: the development of modern transdermal drug delivery systems and future trends. Skin Pharm. Physiol. **26**, 331–342 (2013)
3. H. Trommer, R. Neubert, Overcoming the stratum corneum: the modulation of skin penetration. Skin Pharmacol. Physiol. **19**, 106–121 (2006)
4. S. Becker, B. Zorec, D. Miklavčič, N. Pavšelj: Transdermal transport pathway creation: electroporation pulse order. Math. Biosci. **257**, 60–68 (2014)
5. Y.N. Kalia, A. Naik, J. Garrison, R.H. Guy, Iontophoretic drug delivery. Adv. Drug Deliv. Rev. **56**, 619–658 (2004)
6. G. Pontrelli, F. de Monte, A two-phase two-layer model for transdermal drug delivery and percutaneous absorption. Math. Biosci. **257**, 96–103 (2014)
7. L. Simon, Timely drug delivery from controlled-release devices: Dynamic analysis and novel design concepts. Math. Biosci. **217**, 151–158 (2009)
8. Y.N. Kalia, R.H. Guy, Modeling transdermal drug release. Adv. Drug Del. Rev. **48**, 159–172 (2001)
9. L. Simon, A.N. Weltner, Y. Wang, B. Michniak, A parametric study of iontophoretic transdermal drug-delivery systems. J. Membr. Sci. **278**, 124–132 (2006)
10. T. Gratieri, Y. Kalia, Mathematical models to describe iontophoretic transport in vitro and in vivo and the effect of current application on the skin barrier. Adv. Drug Deliv. Rev. **65**, 315–329 (2013)
11. G. Pontrelli, F. de Monte, A multi-layer porous wall model for coronary drug-eluting stents. Int. J. Heat Mass Trans. **53**, 3629–3637 (2010)
12. G. Pontrelli, M. Lauricella, J.A. Ferreira, G. Pena, Iontophoretic transdermal drug delivery: a multi-layered approach. Math. Med. Biol. online (2016)
13. R. Collins, The choice of an effective time constant for diffusive processes in finite systems. J. Phys. D Appl. Phys. **13**, 1937–1947 (1980)
14. M.A. Ashburn, L.L. Ogden, J. Zhang, G. Love, S.V. Basta, The pharmacokinetics of transdermal fentanyl delivered with and without controlled heat. J. Pain **4**, 291–297 (2003)
15. L. Simon, Analysis of heat-aided membrane-controlled drug release from a process control perspective. Int. J. Heat Mass Trans. **50**, 2425–2433 (2007)
16. Y. Song, S.K. Li, K.D. Peck, H. Zhu, A. Ghanem, W.I. Higuchi, Human epidermal membrane constant conductance iontophoresis: alternating current to obtain reproducible enhanced permeation and reduced lag times of a nonionic polar permeant. Int. J. Pharm. **232**, 45–57 (2002)
17. A. Luzardo-Alvarez, M.B. Delgado-Charro, J. Blanco-Mendez, Iontophoretic delivery of ropinirole hydrochloride: effect of current density and vehicle formulation. Pharm. Res. **18**, 1714–1720 (2001)
18. A.K. Nugroho, O. Della Pasqua, M. Danhof, J.A. Bouwstra, Compartmental modeling of transdermal iontophoretic transport II: in vivo model derivation and application. Pharm. Res. **22**, 335–346 (2005)
19. L. Simon, *Control of Biological and Drug-Delivery Systems for Chemical, Biomedical, and Pharmaceutical Engineering* (Wiley, Hoboken, NJ, 2013)

20. Y.G. Anissimova, Mathematical models for skin toxicology. Expert Opin. Drug Metab. Toxicol. **10**, 551–560 (2014)
21. K. Tojo, *Mathematical models of transdermal and topical drug delivery* (Biocom Systems Inc., Fukuoka, Japan, 2005)
22. P.F. Millington, R. Wilkinson, Skin Cambridge University Press, 2009
23. S. Becker, Transport modeling of skin electroporation and the thermal behavior of the stratum corneum. Int. J. Thermal Sci. **54**, 48–61 (2012)
24. M. Fernandes, L. Simon, N.W. Loney, Mathematical modeling of transdermal drug deliverysystems: analysis and applications. J. Membr. Sci. **256**, 184–192 (2005)
25. J.M. Nitsche, G.B. Kasting, A microscopic multiphase diffusion model of viable epidermis permeability. Biophys. J. **104**, 2307–2320 (2013)